発表者氏名	論文タイトル名	発表誌名	巻号	ページ	出版年
Shimada S, Shimojima K, Masuda T, Nakayama Y, Kohji T, Tsukamoto H, Matsubasa T, Oka A, Yamamoto T.	*MLC1* mutations in Japanese patients with megalencephalic leukoencephalopathy with subcortical cysts.	Hum Genome Variation	1	14019	2014
Abe Y, Kobayashi S, Wakusawa K, Tanaka S, Inui T, Yamamoto T, Kunishima S, Haginoya K.	Bilateral periventricular nodular heterotopia with megalencephaly: a case report.	J Child Neurol	29	818-822	2014
Kobayashi S, Onuma A, Inui T, Wakusawa K, Tanaka S, Shimojima K, Yamamoto T, Haginoya K.	Clinical course and images of four familial cases of Allan-Herndon-Dudley syndrome with a novel monocarboxylate transporter 8 gene mutation.	Pediatr. Neurol	51	414-416	2014
Ogura K, Takeshita K, Arakawa C, Shimojima K, Yamamoto T.	Neuropsychological profiles of patients with 2q37.3 deletion associated with developmental dyspraxia.	Am J Med Genet B	165B	684-690	2014
Yamamoto T, Shimojima K, Shimada S, Yokochi K, Yoshitomi S, Yanagihara K, Imai K, Okamoto N.	Clinical impacts of genomic copy number gains at Xq28.	Hum Genome Variation	1	14001	2014
Shimada S, Hirano Y, Ito S, Oguni H, Nagata S, Shimojima K, Yamamoto T.	A novel *KCNT1* mutation in a Japanese patient with epilepsy of infancy with migrating focal seizures.	Hum Genome Variation	1	14027	2014
Okumura A, Yamamoto T, Miyajima M, Shimojima K, Kondo S, Abe S, Ikeno M, Shimizu T.	3p interstitial deletion including *PRICKLE2* in identical twins with autistic features.	Pediatr Neurol	51	730-733	2014

発表者氏名	論文タイトル名	発表誌名	巻号	ページ	出版年
Okoshi Y, Hayashi M, Kanda S, Yamamoto T.	An autopsy case of microencephaly, bizarre putaminal lesion, and cerebellar atrophy with heart and liver diseases.	Brain Dev	36	707-710	2014
山本俊至, 下島圭子	iPS細胞(幹細胞)を用いる医療の近未来	遺伝子医学MOOK別冊「今さら聞けない『遺伝医学』」メディカルドゥ		pp173-181	2014
山本俊至	出生前診断に用いられる遺伝子検査-マイクロアレイの考え方-	産婦人科の実際	63	1185-1190	2014

Ⅳ. 研究成果の刊行物・別刷

OPEN

Citation: Human Genome Variation (2014) 1, 14019; doi:10.1038/hgv.2014.19

www.nature.com/hgv

DATA REPORT

MLC1 mutations in Japanese patients with megalencephalic leukoencephalopathy with subcortical cysts

Shino Shimada[1,2], Keiko Shimojima[1], Teruaki Masuda[3], Yoshiaki Nakayama[4], Toshihiko Kohji[5], Hiroko Tsukamoto[6], Tadashi Matsubasa[7], Akira Oka[8] and Toshiyuki Yamamoto[1]

Megalencephalic leukoencephalopathy with subcortical cysts (MLC) is an autosomal recessive neurological disorder manifesting early onset macrocephaly and delayed-onset neurological deterioration. Characteristic radiological findings revealed by brain magnetic resonance imaging are the most important factors for obtaining a clinical diagnosis. In this study, we analyzed the causative gene, *MLC1*, in seven unrelated Japanese patients. The most common mutation in our study was p.S93L; this mutation was observed in 11 alleles (78.6%). The second most common mutation, p.A275D, was observed in two alleles (14.3%). A novel single-nucleotide deletion, c.578delG (p.V194Sfs*2), was identified in one allele. As the clinical severities of patients with MLC were variable even among those sharing identical genotypes, this condition may be modified by environmental factors, modifier genes or epigenetic factors.

Human Genome Variation (2014) **1**, 14019; doi:10.1038/hgv.2014.19; published online 30 October 2014

Megalencephalic leukoencephalopathy with subcortical cysts (MLC, MIM #604004) is an autosomal recessive neurological disorder first described by van der Knaap *et al.*[1] that is characterized by early onset macrocephaly and delayed-onset neurological deterioration.[1] Patients with MLC show macrocephaly during the first year of life, followed by slowly progressive deterioration of motor functions with ataxia and spasticity. In such cases, brain magnetic resonance imaging (MRI) shows diffuse signal abnormality in the white matter of the cerebral hemisphere, and subcortical cysts are often observed in the anterior-temporal region and/or in the front-parietal area. The causative gene, *MLC1* (MIM #605908), was first identified in 2001 and maps to chromosome band 22q13.33; this gene contains 12 exons.[2] *MLC1* mutations have been observed in 75% of patients with MLC.[3] Herein, we report the result of an ongoing study to obtain a genetic diagnosis for *MLC1*.

This study was approved by the Ethics Committee of Tokyo Women's Medical University. After obtaining written informed consent from patients or their families, blood samples were obtained from patients with a clinical diagnosis of MLC. The diagnosis was made based on previously defined criteria.[1,4] Genomic DNA was extracted from blood samples using the QIAamp DNA Extraction Kit (QIAGEN, Hamburg, Germany). Parental samples were also obtained to determine inheritance. All exons of *MLC1* were genotyped using standard Sanger sequencing.

We identified three types of *MLC1* mutations in seven unrelated Japanese patients with MLC (Table 1). Eleven alleles contained the c.278C>T (p.S93L) missense mutation (Supplementary Figure 1) in exon 4 (78.6%), and all patients had p.S93L in either of the alleles (Table 1). Patients 1–4 showed homozygous patterns of p.S93L, and the remaining three patients were compound heterozygous for the mutation and one of other mutations. This mutation has been previously reported in individuals from Japan, Turkey and Finland.[2,5,6] Tsujino *et al.*[6] reported that p.S93L is a common mutation in Japanese patients with MLC, with 85.7% of patients and 71.4% alleles showing this mutation.[6] This finding was also confirmed in the present study. Although we did not analyze parental origins in patients 1–4 due to lack of parental samples, parental consanguinities in patients 1–3 and the high frequency of p.S93L suggest that these patients would be homozygous for p.S93L.

The second most common mutation, c.824C>A (p.A275D) in exon 10 (Supplementary Figure 1), was observed in two alleles (14.3%) from patients 5 and 7 (Table 1). Compound heterozygosity was confirmed in these two patients because p.S93L and p.A275D were identified in either of the parents independently. Although this mutation was reported previously by Montagna *et al.*,[7] this is the first report in Japanese patients.

A single-nucleotide deletion, c.578delG (p.V194Sfs*2) (Supplementary Figure 1), was identified in exon 7 in patient 6. To the best of our knowledge, this is a novel mutation. The mother of patient 6 was a carrier of p.S93L (heterozygous of p.S93L); however, the origin of c.578delG was unknown due to lack of a sample from his father. This deletion causes a frameshift mutation and creates a premature termination codon, leading to nonsense-mediated decay. As a consequence, this likely leads to a loss of function of *MLC1*. Such single-nucleotide deletions are rare in *MLC1*.

In the present study, all patients showed brain MRI abnormalities consistent with diffuse white matter abnormalities (Figure 1). Although most of the patients showed detectable subcortical cysts, particularly in anterior-temporal regions (Figure 1), some were too small to be detected in the regular images. The MLC

[1]Tokyo Women's Medical University Institute for Integrated Medical Sciences, Tokyo, Japan; [2]Department of Pediatrics, Tokyo Women's Medical University, Tokyo, Japan; [3]Department of Neurology, Kumamoto Saisyunsou National Hospital, Koshi, Japan; [4]Department of Neurology, Wakayama Medical University, Wakayama, Japan; [5]Department of Pediatrics, Musashino Red Cross Hospital, Musashino, Japan; [6]Department of Pediatrics, Sumitomo Hospital, Osaka, Japan; [7]Kumamoto-Ashikita Medical Center for Severe Motor and Intellectual Disabilities, Kumamoto, Japan and [8]Department of Pediatrics, University of Tokyo, Tokyo, Japan.
Correspondence: T Yamamoto (yamamoto.toshiyuki@twmu.ac.jp)
Received 6 August 2014; revised 27 August 2014; accepted 27 August 2014

Table 1. Summaries of the clinical information of the patients and the results of mutation analyses

Patient	Gender	Present age (y/m)	Onset age (y/m)	First symptom	Present status	Consanguinity	Mutations	Parental origins	Provoking event	Macrocephaly/ OFC[a] (measured age)	Seizures (onset age) (y/m)
1	F	55 y	1 y 10 m	Seizure	Bedridden	+	S93L/S93L	Not confirmed	Head trauma at 18 m	+ 58.5 cm (55 y)	+ (22 m)
2	F	51 y	41 y	Cognitive impairment	Intellectual disability Spasticity	+	S93L/S93L	Not confirmed	–	– 58 cm (51 y)	+ (47 y)
3	F	36 y	1 y 6 m	Macrocephaly	Bedridden	+	S93L/S93L	Not confirmed	Head trauma at 2 y	+ 54 cm (1 y) 62 cm (15 y)	+ (2 y)
4	F	31 y	1 y 3 m	Seizure	Intellectual disability	–	S93L/S93L	Not confirmed	Fever at 15 m	+ NI	+ NI
5	F	18 y	2y	Motor disability	Inability to walk	–	S93L/A275D	Confirmed	–	– 58 cm (18 y)	–
6	M	11 m	11 m	Macrocephaly	NA	–	S93L/V194Sfs*2	Not confirmed	–	+ 50.3 cm (11 m; +2.9 s.d.)	–
7	F	9 m	9 m	Macrocephaly	NA	–	S93L/A275D	Confirmed	–	+ 49.5 cm (9 m; +2.5 s.d.)	–

Abbreviations: F, female; M, male; m, months; NI, no detailed information; s.d., standard deviation; y, years.
[a]Mean OFC for adult Japanese females is 54.6 cm (the third percentile = 52.0 cm, the 97th percentile = 58.1 cm).

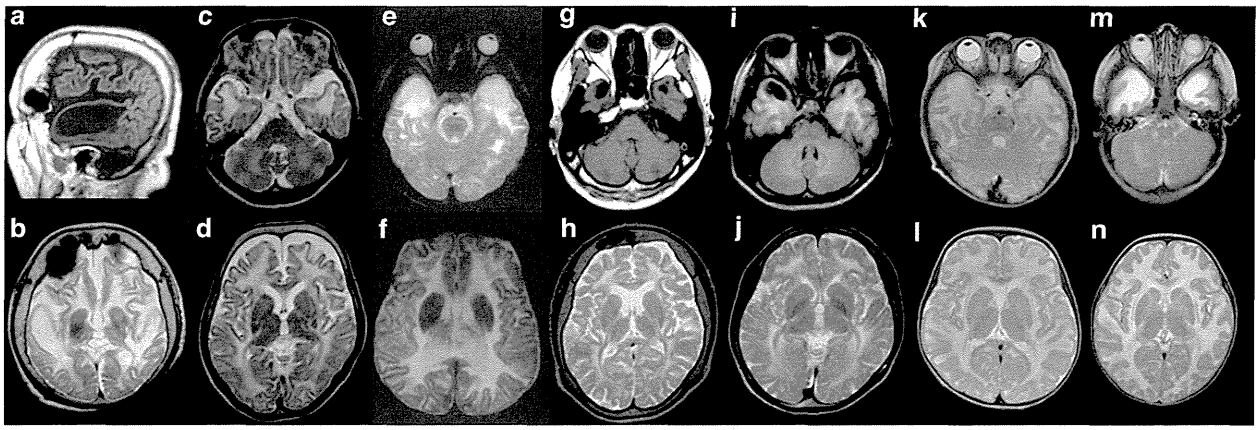

Figure 1. Brain magnetic resonance imaging findings. (**a** and **b**) Patient 1 examined at 55 years of age. The T1-weighted sagittal image (**a**) shows a subcortical cyst in the anterior-temporal region, and diffuse volume loss of the cerebrum is noted (**b**). (**c** and **d**) Patient 2 at 51 years of age. Although subcortical cysts are too small to be detected in the anterior-temporal regions (**c**), mild volume loss of the cerebrum is detectable (**d**). (**e** and **f**) Patient 3 at 16 years of age. (**g** and **h**) and patient 4 at 30 years of age. The T1-weighted axial image (**g**) shows subcortical cysts in the anterior-temporal regions. (**i** and **j**) Patient 5 at 18 years of age. An asymmetric subcortical cyst in the right anterior-temporal regions is noted in the T1-weighted axial image (**i**). (**k** and **l**) Patient 6 at 11 months of age. (**m** and **n**) patient 7 at 9 months of age. The T2-weighted axial images indicate high intensity in the white matter in all patients (**b**–**f**, **h** and **j**–**n**). Subcortical cysts in the anterior-temporal regions are detectable in some of the T2-weighted axial images (**e** and **m**).

patients could be classified into two groups according to age, that is, infant patients and patients older than the teenage years. Two infant patients were diagnosed with MLC as a result of examination for macrocephaly; no neurological findings were observed in either of these two patients at the time of genetic diagnosis.

In comparison, the older patients showed impaired motor and/or intellectual disability and required supports for daily life. Macrocephaly was observed in only two of the five older patients (2/5). The clinical courses and prognoses of these patients were variable. The onset of MLC in the four patients with the p.S93L homozygous mutation was variable, ranging from 15 months to 41 years. Patient 1, who was homozygous for p.S93L, was severely impaired and bedridden from the age of 4. On the other hand, patient 2 showed only mild cognitive and memory deficit and suffered seizures followed by weakness of the extremities at 47 years of age. This type of patient with a good long-term prognosis was also reported by Koyama *et al.*[8] Therefore, this may not necessarily indicate that p.S93L is the mutation causing severe neurological prognosis.

In MLC patients, provoked events are often observed after high fever and head trauma. We observed such provoked events in three patients (Table 1). Because the clinical severities of patients with MLC varied even among patients sharing identical genotypes, disease prognosis may be modified by environmental factors including fever, head trauma, unknown modifier genes, and epigenetic factors.

HGV DATABASE

The relevant data from this Data Report are hosted at the Human Genome Variation Database at http://dx.doi.org/10.6084/m9.figshare.hgv.515, http://dx.doi.org/10.6084/m9.figshare.hgv.517,

http://dx.doi.org/10.6084/m9.figshare.hgv.519, http://dx.doi.org/10.6084/m9.figshare.hgv.521.

ACKNOWLEDGEMENTS

We acknowledge the Collaborative Research Supporting Committee of the Japanese Society of Child Neurology (14-3) for promoting this study. This work was supported by a Grant-in-Aid for Scientific Research from Health Labor Sciences Research Grants from the Ministry of Health, Labor and Welfare, Japan (TY).

COMPETING INTERESTS

The authors declare no conflict of interest.

REFERENCES

1 van der Knaap MS, Barth PG, Stroink H, van Nieuwenhuizen O, Arts WF, Hoogenraad F *et al.* Leukoencephalopathy with swelling and a discrepantly mild clinical course in eight children. *Ann Neurol* 1995; **37**: 324–334.
2 Leegwater PA, Yuan BQ, van der Steen J, Mulders J, Konst AA, Boor PK *et al.* Mutations of MLC1 (KIAA0027), encoding a putative membrane protein, cause megalencephalic leukoencephalopathy with subcortical cysts. *Am J Hum Genet* 2001; **68**: 831–838.
3 Ilja Boor PK, de Groot K, Mejaski-Bosnjak V, Brenner C, van der Knaap MS, Scheper GC *et al.* Megalencephalic leukoencephalopathy with subcortical cysts: an update and extended mutation analysis of MLC1. *Hum Mutat* 2006; **27**: 505–512.
4 van der Knaap MS, Boor I, Estevez R. Megalencephalic leukoencephalopathy with subcortical cysts: chronic white matter oedema due to a defect in brain ion and water homoeostasis. *Lancet Neurol* 2012; **11**: 973–985.
5 Saijo H, Nakayama H, Ezoe T, Araki K, Sone S, Hamaguchi H *et al.* A case of megalencephalic leukoencephalopathy with subcortical cysts (van der Knaap disease): molecular genetic study. *Brain Dev* 2003; **25**: 362–366.
6 Tsujino S, Kanazawa N, Yoneyama H, Shimono M, Kawakami A, Hatanaka Y *et al.* A common mutation and a novel mutation in Japanese patients with van der Knaap disease. *J Hum Genet.* 2003; **48**: 605–608.
7 Montagna G, Teijido O, Eymard-Pierre E, Muraki K, Cohen B, Loizzo A *et al.* Vacuolating megalencephalic leukoencephalopathy with subcortical cysts: functional studies of novel variants in MLC1. *Hum Mutat* 2006; **27**: 292.
8 Koyama S, Kawanami T, Arawaka S, Wada M, Kato T. A Japanese adult case of megalencephalic leukoencephalopathy with subcortical cysts with a good long-term prognosis. *Intern Med* 2012; **51**: 503–506.

Supplementary Information for this article can be found on the *Human Genome Variation* website (http://www.nature.com/hgv)

Journal of Human Genetics (2015) 60, 631–635

www.nature.com/jhg

SHORT COMMUNICATION

Novel compound heterozygous *LIAS* mutations cause glycine encephalopathy

Yoshinori Tsurusaki[1], Ryuta Tanaka[2], Shino Shimada[3], Keiko Shimojima[3], Masaaki Shiina[4], Mitsuko Nakashima[1], Hirotomo Saitsu[1], Noriko Miyake[1], Kazuhiro Ogata[4], Toshiyuki Yamamoto[3] and Naomichi Matsumoto[1]

Glycine encephalopathy (GCE) is a rare autosomal recessive disorder caused by defects in the glycine cleavage complex. Here we report a patient with GCE and elevated level of glycine in both the serum and the cerebrospinal fluid. Trio-based whole-exome sequencing identified novel compound heterozygous mutations (c.738-2A>G and c.929T>C (p.Met310Thr)) in *LIAS*. To date, three homozygous mutations have been reported in *LIAS*. All previously reported GCE patients also show elevated level of serum glycine. Our data further supports *LIAS* mutations as a genetic cause for GCE.
Journal of Human Genetics (2015) **60**, 631–635; doi:10.1038/jhg.2015.72; published online 25 June 2015

INTRODUCTION

Glycine encephalopathy (GCE) (MIM 605899), also known as nonketotic hyperglycinemia, is a rare autosomal recessive disorder of the glycine cleavage system[1] that results in elevated glycine levels in body fluids. GCE is genetically caused by mutations in *AMT* (MIM 238310), *GLDC* (MIM 238300) or *GCSH* (MIM 238330), which encode T-, P- or H-protein, respectively, and together with L-protein constitute the glycine cleavage enzyme.[2–4] Most GCE patients have *GLDC* mutations.[5] Recently, *GLRX5* (MIM 609588), *BOLA3* (MIM 613183) and *LIAS* (MIM 607031) were identified as causative mutant genes for GCE.[6,7] *LIAS* encodes lipoic acid synthetase, a [4Fe-4S]-type iron–sulfur cluster-dependent enzyme that acts as a prosthetic group on H-protein, which is localized within the mitochondria.[8] *GLRX5* and *BOLA3* are iron–sulfur cluster biosynthesis genes.[8] All GCE patients showed elevated level of glycine in the serum, but it is only slightly increased in the cerebrospinal fluid, or even normal, in some GCE patients.[6] In this study, we report a GCE individual with novel compound heterozygous mutations in *LIAS*.

PATIENTS AND METHODS

Case report

A 21-year-old female patient was born to healthy nonconsanguineous parents. Her birth weight was 2954 g (mean), length 48.5 cm (mean) and occipitofrontal circumference 33.8 cm (75th percentile). Her initial development was normal until 18 months. Her elder sister died of herpes simplex virus encephalitis at the age of 18 months. Her elder brother is healthy.

At the age of 19 months, she suffered from an upper respiratory infection. Three days later, she vomited, became excited and then drowsy, and showed chorea-like involuntary movements. She was instantly admitted to the intensive care unit. Magnetic resonance imaging of the brain showed no abnormality (Figure 1). Her cerebrospinal fluid was examined, which showed normal results. Two weeks later, high blood glycine levels were noted (1545 nmol ml^{-1}, normal range 179–587 nmol ml^{-1}), which are still present (Table 1). Her cerebrospinal fluid glycine levels were also high: 45.5 nmol ml^{-1} (normal range 1.6–19.5 nmol ml^{-1}; Table 1). Ketourine was not found. Three months later, magnetic resonance imaging of the brain showed high-intensity areas at the caudate nucleus and the putamen, which spread into the deep white matter (Figure 1).

At present, her height is 156 cm (25–50th percentile), weight 47.3 kg (10–25th percentile) and the occipitofrontal circumference 52.5 cm (<3rd percentile). She is now bedridden. Tube feeding has been required since 19 months of age. She speaks no meaningful words and shows no eye contact. Myoclonic movements and intractable epilepsy have been observed. Magnetic resonance imaging of the brain shows brain atrophy, especially in the white matter (Figure 1). The institutional review boards of Yokohama City University School of Medicine and Tokyo Women's Medical University approved the study. Informed consent was obtained from the family.

Whole-exome sequencing

DNA from the patient and her parents were analyzed by whole-exome sequencing, as previously described.[9] Genomic DNA was captured using the SureSelect Human All Exon v5 (50 Mb) Kit (Agilent Technologies, Santa Clara, CA, USA). Captured DNA was sequenced on a HiSeq2500 (Illumina, Inc., San Diego, CA, USA) with 101 bp paired-end reads and 7 bp index reads. Image analysis and base calling were performed by sequence control software real-time analysis and CASAVA software (v1.8) (Illumina, Inc.). Quality-controlled reads were mapped to the human reference genome (UCSC hg19, NCBI build 37.1) using Novoalign (v3.00.02; http://www.novocraft.com/products/novoalign/).

[1]Department of Human Genetics, Yokohama City University Graduate School of Medicine, Yokohama, Japan; [2]Department of Child Health, Institute of Clinical Medicine, University of Tsukuba, Ibaraki, Japan; [3]Institute for Integrated Medical Sciences, Tokyo Women's Medical University, Tokyo, Japan and [4]Department of Biochemistry, Yokohama City University Graduate School of Medicine, Yokohama, Japan
Correspondence: Dr N Matsumoto, Department of Human Genetics, Yokohama City University Graduate School of Medicine, 3-9 Fukuura, Kanazawa-ku, Yokohama 236-0004, Japan.
E-mail: naomat@yokohama-cu.ac.jp
Received 6 February 2015; revised 18 May 2015; accepted 28 May 2015; published online 25 June 2015

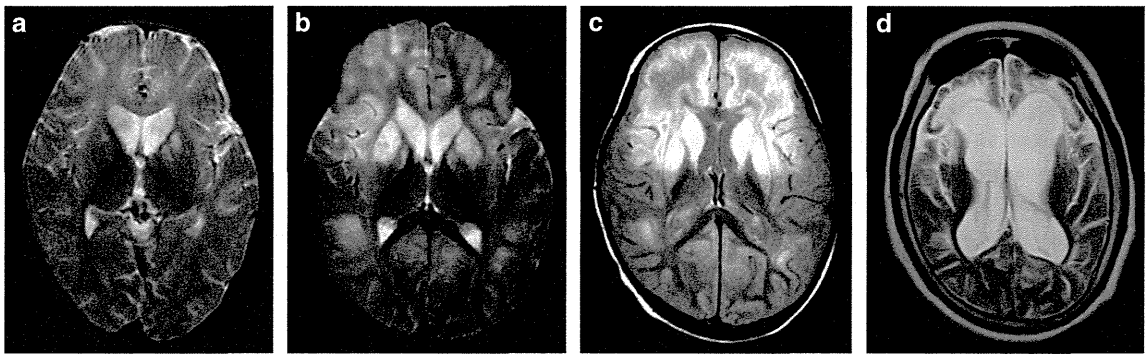

Figure 1 T2-weighted brain magnetic resonance imaging (MRI) of the individual with *LIAS* mutations. (**a**) Examined at disease onset (19 months old). High-intensity areas are present in the caudate nucleus and the putamen. (**b**) Seven days after disease onset. The high-intensity areas have expanded into the white matter, especially in the frontal region. (**c**) One month after disease onset. High-intensity areas are noted not only in the basal nucleus but also in the subcortical white matter, especially in the frontal region. (**d**) At 15 years old. Owing to diffuse cerebral atrophy, the lateral ventricles have expanded. White matter atrophy is predominant in the frontal region.

Table 1 Clinical features of GCE patients with *LIAS* mutations

	This study	*Mayr* et al.,[7]	*Baker* et al.,[6] *(Patient 7)*	*Baker* et al.,[6] *(Patient 8)*
Gene mutation	c.929T>C c.738-2A>G	c.746G>A	c.475_477delGAG insAAA	c.645T>A
Amino acid change	p.M310T Splice site mutation	p.R249H	p.E159K	p.D215E
Plasma glycine (mM; normal range:179–587)	1545	906	890/1035	759
CSF glycine (mM; normal range:1.6–19.5)	45.5	NA	180/94	16
CSF/plasma glycine ratio	0.03	NA	0.20/0.09	0.02
Age	21 Years	4 Years/death	2 Years 8 months/death	14 Years
Onset	19 Months	Third day	Third day	Second day
Initial symptoms	Acute encephalopathy with involuntary movements	Seizure	Hypotonia, seizure	Hypotonia, seizure
Developmental delays	+	NA	+	+
Brain images	Brain atrophy of the especially in the white matter	Multicystic encephalopathy, hydrocephalus *ex vacuo*	Brain atrophy of the cerebrum in both the cortex and the white matter	Normal

Abbreviations: +, present; −, absent; CSF, cerebrospinal fluid; NA, data not available.

After removal of PCR duplications using Picard (v1.55; http://broadinstitute.github.io/picard/), single-nucleotide variants and short insertions and deletions (Indels) were called using Genome Analysis Toolkit (v1.6-5; https://www.broadinstitute.org/gatk/) and were annotated using ANNOVAR (June 2013; http://annovar.openbioinformatics.org/en/latest/).

Prioritization of variants

All variants within exons or ±2 bp from exon–intron boundaries and registered in dbSNP137, the National Heart Lung and Blood Institute Exome Sequencing Project Exome Variant Server (NHLBI-ESP 6500), Human Genome Variation Database, or our in-house (exome data from 575 Japanese individuals) databases, as well as synonymous variants, were removed. Variants were confirmed by Sanger sequencing with an ABI PRISM 3500xl or ABI3130xl autosequencer (Life Technologies, Carlsbad, CA, USA).

Structural modeling

Crystal structure of lipoyl synthase 2 from *Thermosynechococcus elongatus* (PDB code 4U0P)[10] was selected as the most similar model to human LIAS by Phyre2 protein fold recognition server.[11]

Reverse transcription-PCR and nonsense-mediated mRNA decay analysis

Lymphoblastoid cell lines derived from the patient and a healthy control were established. After incubation with 1.5 µl of dimethyl sulfoxide(as a negative control) or 1.5 µl of the protein synthesis inhibitor cycloheximide (100 mg ml^{-1} in dimethyl sulfoxide) (Sigma-Aldrich, St Louis, MO, USA) for 4 h. Total RNA was isolated from treated lymphoblastoid cells using the RNeasy Plus Mini Kit (Qiagen, Hilden, Germany) and was used for reverse transcription with the Super Script III First-Strand Synthesis System (Life Technologies). One microliter of synthesized cDNA was amplified by PCR. PCR products were electrophoresed on a 5%–20% gradient polyacrylamide gel, stained with ethidium bromide and quantitatively measured using a FluorChem 8900 (Alpha Innotech, San Leandro, CA, USA). Three independent experiments were performed. Statistical analyses were performed using analysis of variance. Each PCR band was cloned into the pCR4-TOPO vector (Life Technologies) and sequenced using ABI 3130xl autosequencer.

RESULTS

The mean read depth against RefSeq coding sequence was 89.08–123.7 reads, with 92.2%–94.7% of coding sequence covered by 20 or more

reads. We focused on *de novo* and recessive mutations. We only found novel compound heterozygous mutations in *LIAS*. Sanger sequencing confirmed that c.738-2A>G was transmitted from her mother and c.929T>C (p.Met310Thr) from her father (Figure 2a and Table 1). These two mutations were not registered in dbSNP137, National Heart Lung and Blood Institute Exome Sequencing Project Exome Variant Server (NHLBI-ESP 6500), Human Genome Variation Database, or our in-house 575 Japanese control exome databases. The missense mutation (p.Met310Thr) was predicted as damaging by SIFT (http://sift.jcvi.org/), Polyphen-2 (http://genetics.bwh.harvard.edu/pph2/) and MutationTaster (http://www.mutationtaster.org/), and was evolutionarily conserved (Figure 2a). Moreover, the p.Met310Thr substitution localizes to the Elp3 domain in an iron–sulfur cluster binding site predicted by SMART (http://smart.embl-heidelberg.de/) (Figure 2a). The splice site mutation (c.738-2A>G) was predicted to abolish an acceptor site by ESEfinder (http://rulai.cshl.edu/cgi-bin/tools/ESE3/esefinder.cgi), NetGene2 (http://www.cbs.dtu.dk/services/NetGene2/) and BDGP (http://www.fruitfly.org/seq_tools/splice.html).

We mapped the mutation site (p.Met310Thr) on the crystal structure of lipoyl synthase 2 from *T. elongatus* (TeLipA2) (PDB code 4U0P),[10] analogous to human LIAS (Met310 in human LIAS corresponds to Leu241 in TeLipA2), to evaluate structural impact of the mutation. The main-chain amide and carbonyl groups of Leu241 (Met310) make hydrogen bonds to adenine ring of 5′-methylthioadenosine, a breakdown product of the *S*-adenosylmethionine (Figure 2b), suggesting that the stability of the main-chain region around Leu241 (Met310) is important in *S*-adenosylmethionine binding. The side chain of Leu241 is involved in a hydrophobic core (Figure 2b) and is considered to contribute to the main-chain stability. Thus, the p.Leu241Thr (p.Met310Thr) mutation is likely to impair the enzymatic activity due to destabilized *S*-adenosylmethionine binding.

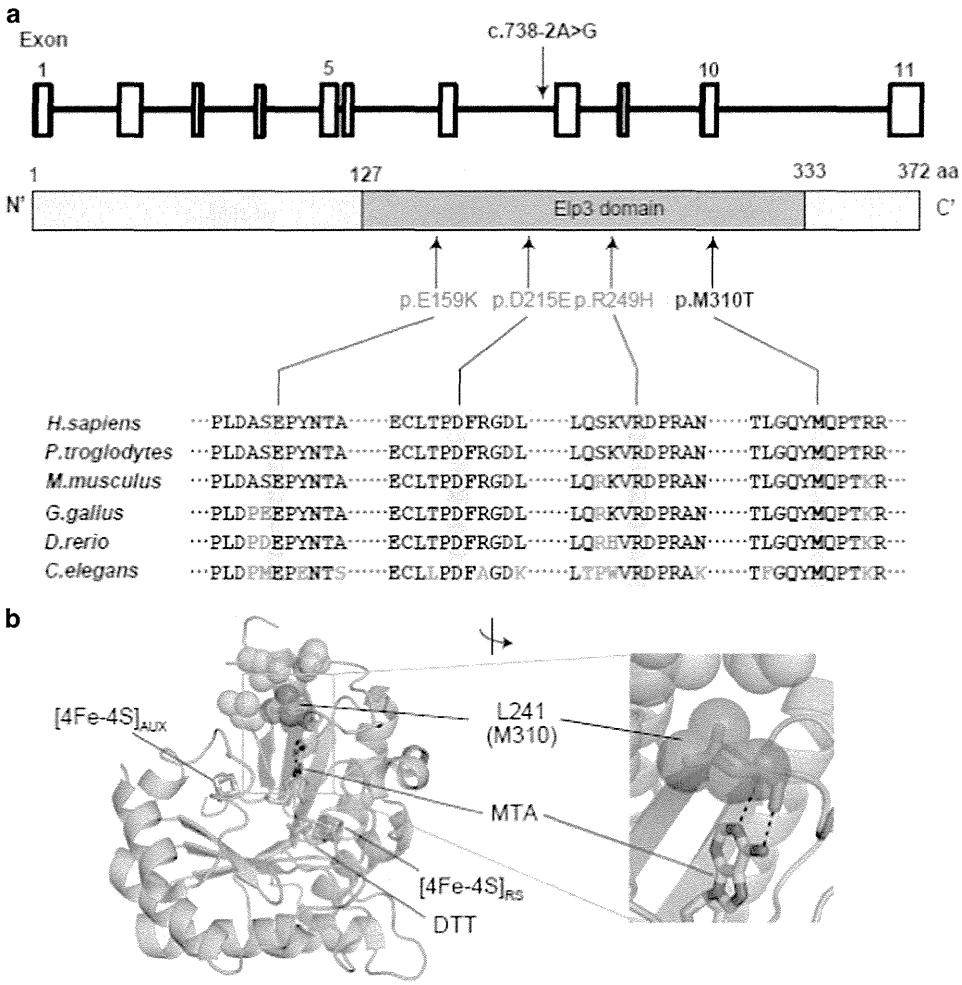

Figure 2 All the *LIAS* mutations. (**a**) *LIAS* missense mutations. Novel compound heterozygous mutations (c.738-2A>G and c.929T>C (p.M310T)) identified in the patient. The upper and middle panels show the *LIAS* gene structure that comprises 11 exons. LIAS contains an Elp3 domain, predicted by SMART. The lower panel shows evolutionary conservation of the mutated amino acid through six different species. The altered nucleotides are highlighted in gray boxes. Three previously reported mutations (p.R249H, p.E159K and p.D215E) are highlighted in gray. (**b**) Mutation mapping on the crystal structure of lipoyl synthase 2 from *T. elongatus* (PDB code 4U0P), which is analogous to human LIAS. The mutation site is shown as sticks with translucent spheres in red in the whole (left) and the close-up (right) views of the enzyme structure. 5′-methylthioadenosine (MTA), [4Fe-4S] clusters and dithiothreitol (DTT) are depicted in color-coded sticks: green for C, red for O, blue for N, yellow for S and orange for Fe. Some hydrophobic side chains forming a core with Leu241 are shown as translucent spheres. The amino acid number in the parentheses is that for human LIAS. Black dashed lines indicate hydrogen bonds. A full color version of this figure is available at the *Journal of Human Genetics* journal online.

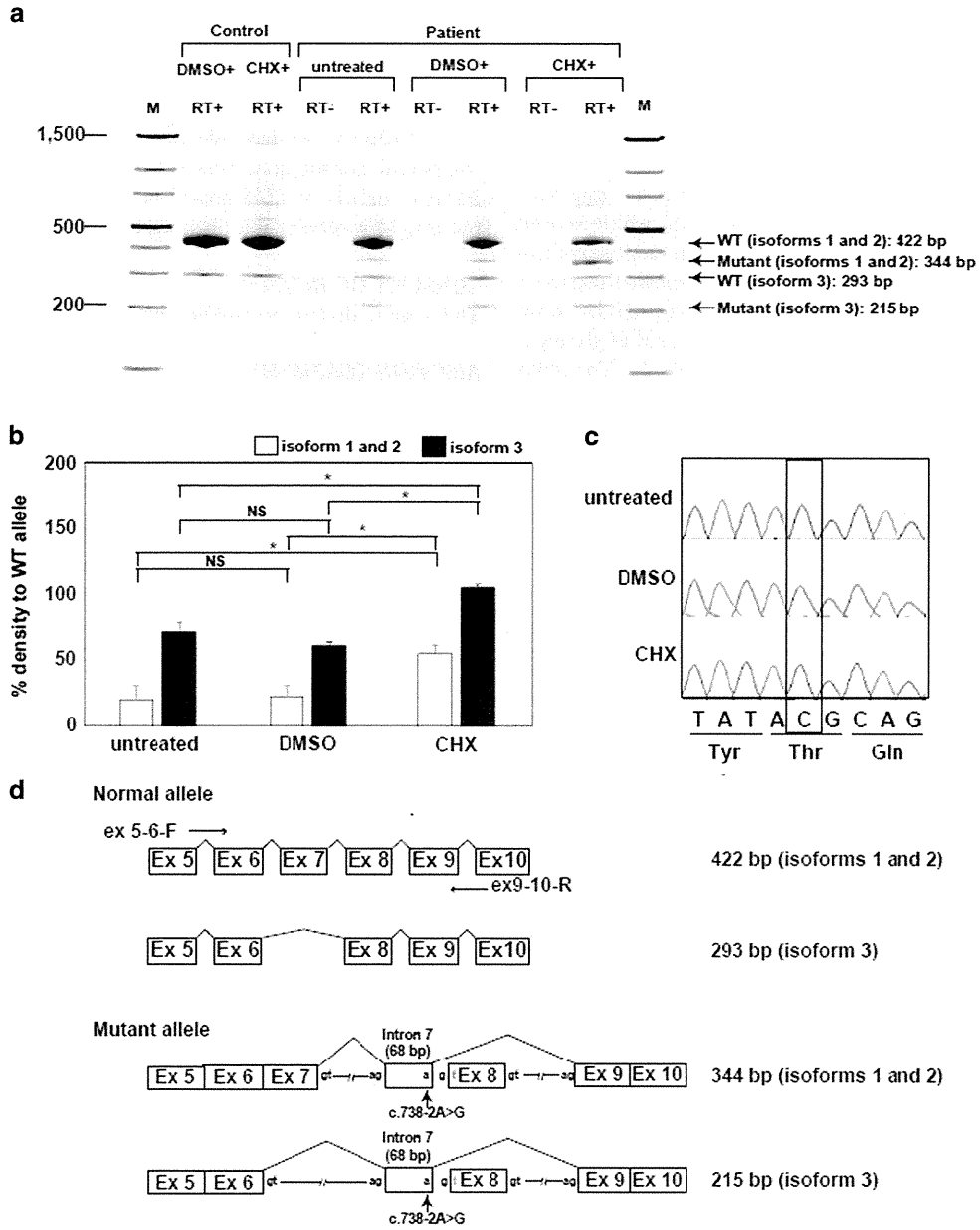

Figure 3 A splice site *LIAS* mutation. (**a**) Reverse transcription-PCR (RT-PCR) analysis showing two PCR products (422-bp (isoforms 1 and 2) and 293-bp (isoform 3)) were observed in a healthy control individual. By contrast, a 344-bp product (corresponding to isoforms 1 and 2) and a 215-bp product (corresponding to isoform 3) were detected in cycloheximide (CHX)-treated cells from the patient at a higher level compared with untreated and dimethyl sulfoxide (DMSO)-treated cells. (**b**) Densitometric data of the RT-PCR products represented as mean ± s.d. $*P<0.05$ by analysis of variance (ANOVA). NS, not significant. (**c**) Sequencing of the 422-bp wild type (WT) product only found missense mutation allele based on the electropherogram. (**d**) Schematic presentation of RT-PCR products. Sequencing of the 344-bp product showed a 68-bp insertion from intron 7 and exon 8 skipping, producing a premature stop codon at amino acid position 250. Sequencing of the 215-bp product showed a 68-bp insertion from intron 7 and exons 7 and 8 skipping, producing a premature stop codon at amino acid position 207. M, molecular size marker; WT, wild type. A full color version of this figure is available at the *Journal of Human Genetics* journal online.

To examine the mutational effects of c.738-2A>G, reverse transcription-PCR was performed. Two PCR products (422-bp (isoforms 1 and 2) and 293-bp (isoform 3)) were observed in a healthy control individual regardless of the cycloheximide treatment (Figure 3a). By contrast, a 344-bp product (corresponding to isoforms 1 and 2) and a 215-bp product (corresponding to isoform 3) were newly detected from cycloheximide-treated cells from the patient at a higher level compared with untreated and dimethyl sulfoxide-treated cells, strongly indicating the abnormally spliced allele was subjected to the nonsense-mediated mRNA decay (Figure 3b). In the 422-bp product, only the missense mutation allele was seen in the electropherograms of all untreated, dimethyl sulfoxide- and cycloheximide-treated cells (Figure 3c). Therefore, the normally spliced allele only contained the missense mutation. Sequencing of the 344-bp product showed a 68-bp insertion from intron 7 and exon 8 skipping, producing a premature stop codon at amino acid position 250

(Figure 3d). In addition, sequencing of the 215-bp product confirmed a 68-bp insertion from intron 7 and exons 7 and 8 skipping, producing a premature stop codon at amino acid position 207 (Figure 3d).

DISCUSSION

We report a family with compound heterozygous mutations (c.738-2A>G and c.929T>C (p.M310T)) in *LIAS*, which showed developmental delays, myoclonic movements and intractable epilepsy (Table 1). Magnetic resonance imaging of the brain showed atrophy in the white matter (Figure 1). The patient also showed late-onset involuntary movements such as chorea and elevated level of glycine in both the serum and the cerebrospinal fluid (Table 1). The splice acceptor site mutation leads to the error in splicing of intron 7 and exon 8, with a premature stop codon at amino acid position 250 in isoforms 1 and 2 or 207 in isoform 3. Consequently, the product of this mutant transcript may be subjected to nonsense-mediated mRNA decay (likely as shown in Figure 3) or produce a truncated protein at the Elp3 domain if translated (less likely).

To date, three homozygous mutations (p.R249H, p.E159K and p.D215E) have been reported in *LIAS* patients (Table 1).[6,7] These three missense mutations occur at evolutionarily conserved amino acids in the Elp3 domain (Figure 2a). The three reported patients show early-onset seizures within the first 2–3 days and elevated plasma glycine levels (Table 1). The patient described here shows no seizures and very late disease onset at age of 19 months (Table 1). The variable clinical features in patients with *LIAS* mutations may be associated with the severity of the functional impact on protein lipoylation.[6]

Lias homozygous knockout mice die at the early implantation stage between 7.5 and 9.5 days post coitum, suggesting that *Lias* is essential for embryonic development.[12] The previously reported *LIAS* mutations are all homozygous missense mutations. Lipoamide reduction of lipoylated proteins was severely reduced in two patients (p.Arg249His and p.Glu159Lys) with early infantile lethality (at 2 and 4 years).[6,7] In contrast, one patient (p.Asp215Glu) with hypotonia and seizures showed constant development and residual lipoylated proteins, suggesting that some lipoic acid synthetase activity is retained. Thus, residual lipoic acid synthetase activity may be correlated with phenotypic severity. On the other hand, a glycine level is elevated in all patients. Thus, serum glycine levels may not be correlated with *LIAS* genotypes. Regardless of some biochemical and clinical data, it is difficult to extract clinical difference between our case of heterozygous mutations and reported cases of homozygous missense mutations due to the limited number of patients ($n=4$). Further accumulation of patients with *LIAS* mutations is needed.

Most GCE patients caused by *GLDC* or *AMT* mutations show hypotonia, lethargy and apnea leading to death in the first few days after birth. If they overcome apnea regaining spontaneous respiration, they develop intractable seizures and intellectual disability.[13] All the four patients with *LIAS* mutations including our patient lived after at least 2 years of age. Therefore, *LIAS* mutant phenotype is relatively milder compared with the common GCE.

The acute onset of encephalopathy in our patient is interesting. We assumed that the stressful condition by the upper respiratory infection would have been the trigger of disease progression as sometimes seen in other cases of vanishing white matter.

In conclusion, we have identified for the first time, a patient with compound heterozygous missense and splice site mutations in *LIAS*. Further analysis of *LIAS*-related patients is needed to delineate the phenotypic spectrum and phenotype–genotype correlation.

CONFLICT OF INTEREST

The authors declare no conflicts of interest.

ACKNOWLEDGEMENTS

We thank the patients and their families for their participation in this study. We also thank Nobuko Watanabe for her excellent technical assistance. This work was supported by the Ministry of Health, Labour and Welfare of Japan; the Japan Society for the Promotion of Science (Grants-in-Aid for Scientific Research (A) (B) (C)); the Takeda Science Foundation; the Japan Science and Technology Agency (the fund for Creation of Innovation Centers for Advanced Interdisciplinary Research Areas Program in the Project for Developing Innovation Systems); the Ministry of Education, Culture, Sports, Science and Technology of Japan (the Strategic Research Program for Brain Sciences); and a Grant-in-Aid for Scientific Research on Innovative Areas (Transcription Cycle).

1 Brenton, J. N. & Rust, R. S. Late-onset nonketotic hyperglycinemia with a heterozygous novel point mutation of the GLDC gene. *Pediatr. Neurol.* **50**, 536–538 (2014).
2 Nanao, K., Okamura-Ikeda, K., Motokawa, Y., Danks, D. M., Baumgartner, E. R., Takada, G. *et al.* Identification of the mutations in the T-protein gene causing typical and atypical nonketotic hyperglycinemia. *Hum. Genet.* **93**, 655–658 (1994).
3 Kure, S., Narisawa, K. & Tada, K. Structural and expression analyses of normal and mutant mRNA encoding glycine decarboxylase: three-base deletion in mRNA causes nonketotic hyperglycinemia. *Biochem. Biophys. Res. Commun.* **174**, 1176–1182 (1991).
4 Koyata, H. & Hiraga, K. The glycine cleavage system: structure of a cDNA encoding human H-protein, and partial characterization of its gene in patients with hyperglycinemias. *Am. J. Hum. Genet.* **48**, 351–361 (1991).
5 Kanekar, S. & Byler, D. Characteristic MRI findings in neonatal nonketotic hyperglycinemia due to sequence changes in GLDC gene encoding the enzyme glycine decarboxylase. *Metab. Brain Dis.* **28**, 717–720 (2013).
6 Baker, P. R. 2nd, Friederich, M. W., Swanson, M. A., Shaikh, T., Bhattacharya, K., Scharer, G. H. *et al.* Variant non ketotic hyperglycinemia is caused by mutations in LIAS, BOLA3 and the novel gene GLRX5. *Brain* **137**, 366–379 (2014).
7 Mayr, J. A., Zimmermann, F. A., Fauth, C., Bergheim, C., Meierhofer, D., Radmayr, D. *et al.* Lipoic acid synthetase deficiency causes neonatal-onset epilepsy, defective mitochondrial energy metabolism, and glycine elevation. *Am. J. Hum. Genet.* **89**, 792–797 (2011).
8 Mayr, J. A., Feichtinger, R. G., Tort, F., Ribes, A. & Sperl, W. Lipoic acid biosynthesis defects. *J. Inherit. Metab. Dis.* **37**, 553–563 (2014).
9 Tsurusaki, Y., Koshimizu, E., Ohashi, H., Phadke, S., Kou, I., Shiina, M. *et al. De novo* SOX11 mutations cause Coffin-Siris syndrome. *Nat. Commun.* **5**, 4011 (2014).
10 Harmer, J. E., Hiscox, M. J., Dinis, P. C., Fox, S. J., Iliopoulos, A., Hussey, J. E. *et al.* Structures of lipoyl synthase reveal a compact active site for controlling sequential sulfur insertion reactions. *Biochem. J.* **464**, 123–133 (2014).
11 Kelley, L. A. & Sternberg, M. J. Protein structure prediction on the Web: a case study using the Phyre server. *Nat. Protoc.* **4**, 363–371 (2009).
12 Yi, X. & Maeda, N. Endogenous production of lipoic acid is essential for mouse development. *Mol. Cell. Biol.* **25**, 8387–8392 (2005).
13 Hennermann, J. B., Berger, J. M., Grieben, U., Scharer, G. & Van Hove, J. L. Prediction of long-term outcome in glycine encephalopathy: a clinical survey. *J. Inherit. Metab. Dis.* **35**, 253–261 (2012).

ELSEVIER

Brain & Development 38 (2016) 142–144

BRAIN & DEVELOPMENT
Official Journal of the Japanese Society of Child Neurology

www.elsevier.com/locate/braindev

Case Report

White matter abnormalities in an adult patient with L-2-hydroxyglutaric aciduria

Toshiyuki Yamamoto [a,*], Seiichiro Yoshioka [b], Yoshinori Tsurusaki [c], Shimada Shino [a,d], Keiko Shimojima [a], Yosuke Shigematsu [e], Yoshihiro Takeuchi [b], Naomichi Matsumoto [c]

[a] *Tokyo Women's Medical University Institute for Integrated Medical Sciences, Tokyo, Japan*
[b] *Department of Pediatrics, Shiga Medical University, Ohtsu, Japan*
[c] *Department of Human Genetics, Yokohama City University Graduate School of Medicine, Yokohama, Japan*
[d] *Department of Pediatrics, Tokyo Women's Medical University, Tokyo, Japan*
[e] *Department of Health Science, Faculty of Medical Sciences, University of Fukui, Japan*

Received 7 April 2015; received in revised form 30 April 2015; accepted 30 April 2015

Abstract

L-2-Hydroxyglutaric aciduria (L-2-HGA) is a rare inborn error of metabolism. Mainly, patients with this disorder exhibit neurological symptoms and characteristic neuroradiological findings, such as subcortical white matter abnormalities, which are believed to be caused by the toxicity of the accumulation of L-2-hydroxyglutaric acid. A genotype-first approach of the whole exome sequence was used to identify compound heterozygous mutations, c.584A>G (p.Y195C) and c.772T>C (p.C258R), in *L2HGDH*, the gene responsible for this disorder, in an adult patient with intellectual disability and intractable epilepsy. A retrospective assay confirmed the increased concentrations of 2-hydroxyglutaric acid in the urine. These results suggested that neuroradiological findings of subcortical white matter abnormalities are characteristic of L-2-HGA and that clinical exome sequencing has sufficient power to compensate for insufficient clinical evaluations.

Keywords: L-2-Hydroxyglutaric aciduria (L-2-HGA); *L2HGDH*; Subcortical white matter abnormalities; Genotype-first approach; Clinical exome sequencing

1. Introduction

L-2-Hydroxyglutaric aciduria (L-2-HGA; MIM#236792) is a rare inborn error of metabolism, which involves defects in the metabolism of L-2-hydroxyglutaric acid, which results in increased levels of the acid in the urine. Since the first case was described in 1980 [1], some cases have been reported in Japan [2] and worldwide. The gene responsible for this disorder, *L2HGDH*, which is located on chromosome 14q22.1, was identified in 2004 [1]. The pathogenesis of the accumulation of L-2-hydroxyglutaric acid is unclear, but it is probably toxic to the white matter through myelin vacuolation [3]. Consequently, the neuroradiological findings in these patients are unique, and the subcortical white matter abnormalities can be visualized with brain magnetic resonance imaging (MRI) [4].

Although the diagnosis of an inborn error of metabolism can generally be made by screening of the metabolic

* Corresponding author at: Tokyo Women's Medical University Institute for Integrated Medical Sciences, 8-1 Kawada-cho, Shinjuku-ward, Tokyo 162-8666, Japan. Tel.: +81 3 3353 8112x24013; fax: +81 3 5269 7667.
E-mail address: yamamoto.toshiyuki@twmu.ac.jp (T. Yamamoto).

http://dx.doi.org/10.1016/j.braindev.2015.04.012
0387-7604/

substrate, such an error is often undiagnosed because of phenotypic heterogeneity. Recent advancements in molecular analysis equipment have overcome this dilemma in clinical diagnosis. Some cases with inborn error of metabolism have been diagnosed with genotype-first approach and not by metabolism screening [5,6]. Here, we present a new patient with L-2-HGA who exhibited white matter abnormalities and who was diagnosed by clinical exome sequencing.

2. Patient report

A 33-year-old female patient was born with a birth weight of 2500 g (mean), a length of 47.5 cm (25th–50th centile), and an occipitofrontal circumference (OFC) of 32 cm (10th–20th centile). Her parents were non-consanguineous and healthy. She has four siblings. She started to show recurrent febrile seizures at 7 months. She began to walk with supports at 10 months and to talk with meaningful words at 9 months. Her neurodevelopment was within normal limits until 8 years of age. At that time, she exhibited nonfebrile seizures. Because an electroencephalography showed right-frontal dominant spike and wave discharges, anti-epileptic drugs were prescribed. Subsequently, her psychomotor development gradually delayed. Her generalized tonic seizures were intractable, and several attacks were observed per year. Because her intellectual capacity is at the approximate level of a 5-year-old, she lives in a group home that is supported by welfare.

At 33 years of age, she suddenly showed status epilepticus that was associated with drowsiness and without any trigger. She was immediately transferred to the hospital. Although she recovered consciousness after treatment, a brain MRI revealed abnormal findings in the white matter for the first time (Fig. 1).

At present, her height is 164 cm (90th–97th centile), her weight is 85 kg (>97th centile), and her OFC is 54 cm (10th centile), which indicates that she is obese with a body mass index of 31.6. A physical examination showed no abnormalities. A neurological examination revealed mild ataxia and dystonic posture. After obtaining the molecular diagnosis, combined D-2- and L-2-hydroxyglutaric acid levels in urine were measured using urease-pretreatment of urine, trimethylsilylation, and gas chromatography-mass spectrometry [7]. Although an increased concentration was detected, D-2- and L-2-hydroxyglutaric acids cannot be separated in this method.

3. Molecular analysis

The ethical committee of Tokyo Women's Medical University approved this study. After obtaining written informed consent from the patient's family, blood samples were obtained from the patient and her parents. DNA was extracted from the blood samples using QIAamp DNA extraction kit (QIAGEN GmbH, Hilden, Germany). DNA from the patient and her parents were analyzed with whole exome sequencing as previously described [8].

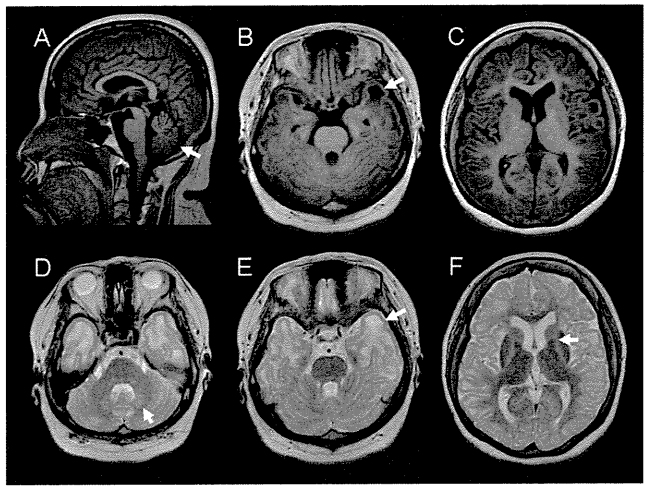

Fig. 1. The results of the brain magnetic resonance imaging that was performed on the patient at 33 years of age. (A) A T1-weighted sagittal image shows remarkable folia of the cerebrum (arrow), indicating mild atrophy. (B and C) T1-weighted axial images. (D–F) T2-weighted axial images. Diffuse subcortical white matter abnormalities are noted in axial images. Some of the subcortical regions (arrows) show cystic changes (B and D). The involvement of the dentate nucleus (arrow) is characteristic (D). Signal high intensity is shown in the anterior and posterior limbs of internal capsule (F). Dilatations of the lateral ventricles and extra-cerebral spaces indicate diffuse brain atrophy.

We focused on *de novo* and recessive mutations. Although there were no *de novo* mutations that have functional relevance to neurological disorders, we identified the following compound heterozygous mutations of *L2HGDH*: c.584A>G (p.Y195C) and c.772T>C (p.C258R). These mutations were transmitted from her father and mother, respectively. Sanger sequencing confirmed these findings (Fig. 2). The c.772T>C mutation is registered in the dbSNP137 SNP database as rs145390085, and it has a frequency of 0.007% in the National Heart, Lung, and Blood Institute Exome Sequencing Project (NHLBI-ESP) 6500 (http://evs.gs.washington.edu/EVS/). The c.584A>G mutation is not registered in the dsSNP137 SNP database, NHLBI-ESP 6500, Human Genetic Variation Browser database (http://www.genome.med.kyoto-u.ac.jp/SnpDB/), or in any of our 575 in-house Japanese control exome databases. The c.584A>G and c.772T>C mutations were predicted to be damaging by SIFT (http://sift.jcvi.org/) scores of 0.00 for both, Polyphen-2 (http://genetics.bwh.harvard.edu/pph2/) scores of 0.986 and 1.000, respectively, and MutationTaster (http://neurocore.charite.de/MutationTaster/) scores of 1.000 for both.

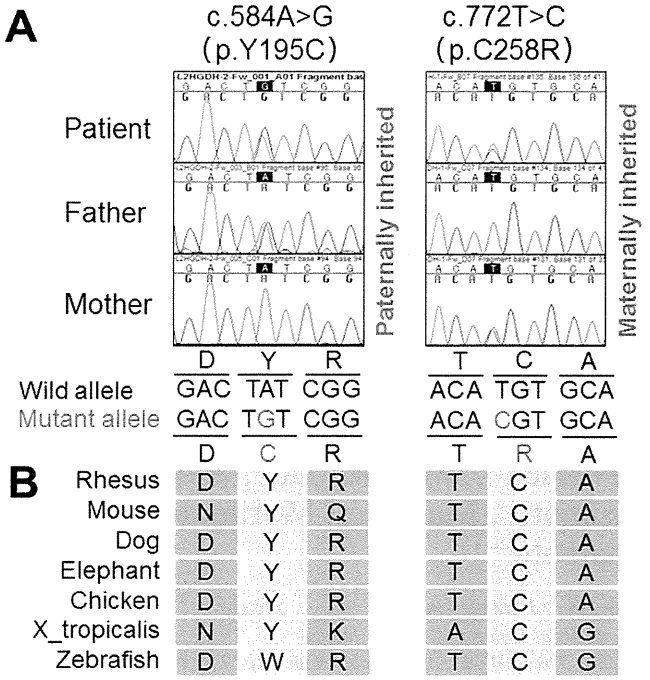

Fig. 2. The results of the molecular analysis. (A) Sanger sequencing confirms compound heterozygous mutations that are transmitted from both parents. (B) The affected amino acids are conserved among mammals.

4. Discussion

In this study, we identified compound heterozygous variants of *L2HGDH* in an adult patient with epilepsy and intellectual disability. The paternally transmitted c.584A>G mutation was previously reported as a disease-causing mutation by Sass et al. [9]. In comparison, the maternally transmitted c.772T>C mutation was registered in the dbSNP database. However, its frequency was extremely low (0.007%), and the prediction software suggested that the consequence of this variant would be damaging. Therefore, we concluded that this variant was pathogenic. Urine screening that was performed after identification of the *L2HGDH* mutations detected an increased concentration of 2-hydroxyglutaric acid in the urine, and a final diagnosis of L-2-HGA was made in this patient.

Although this patient did not show developmental delay in early infancy, she started to show epilepsy and subsequent developmental deterioration at 8 years of age. This clinical course is typical for patients with L-2-HGA [10], but it is not specific and is also rather frequently observed in the histories of patients with intractable epilepsy. From the characteristic white matter abnormalities that were revealed by MRI, which the patient first underwent at 33 years of age after her status epilepticus, we suspected leukoencephalopathy, and we performed genetic screening. Although a diagnosis of L-2-HGA is generally made after findings of highly increased levels of L-2-hydroxyglutaric acid in the urine, a urine screening was never performed in this patient before the exome sequencing results were obtained. Therefore, a brain MRI examination and urine screening should have been performed in the early stages of the disease in this patient. Furthermore, a candidate diagnosis of L-2-HGA might have possibly been obtained after careful evaluation of the characteristic MRI findings [4]. Because there is a report of therapeutic approach using riboflavin, early diagnosis of L-2-HGA would be required [1].

Acknowledgements

We would like to express our gratitude to the patient and her parents for their cooperation. This work was supported by a Grant-in-Aid for Scientific Research from Health Labor Sciences Research Grants from the Ministry of Health, Labor, and Welfare, Japan.

References

[1] Kranendijk M, Struys EA, Salomons GS, Van der Knaap MS, Jakobs C. Progress in understanding 2-hydroxyglutaric acidurias. J Inherit Metab Dis 2012;35:571–87.
[2] Fujitake J, Ishikawa Y, Fujii H, Nishimura K, Hayakawa K, Inoue F, et al. L-2-Hydroxyglutaric aciduria: two Japanese adult cases in one family. J Neurol 1999;246:378–82.
[3] van der Knaap MS, Jakobs C, Hoffmann GF, Nyhan WL, Renier WO, Smeitink JA, et al. D-2-Hydroxyglutaric aciduria: biochemical marker or clinical disease entity? Ann Neurol 1999;45:111–9.
[4] Steenweg ME, Salomons GS, Yapici Z, Uziel G, Scalais E, Zafeiriou DI, et al. L-2-Hydroxyglutaric aciduria: pattern of MR imaging abnormalities in 56 patients. Radiology 2009;251:856–65.
[5] Prada CE, Gonzaga-Jauregui C, Tannenbaum R, Penney S, Lupski JR, Hopkin RJ, et al. Clinical utility of whole-exome sequencing in rare diseases: galactosialidosis. Eur J Med Genet 2014;57:339–44.
[6] Schuster J, Khan TN, Tariq M, Shaiq PA, Mabert K, Baig SM, et al. Exome sequencing circumvents missing clinical data and identifies a BSCL2 mutation in congenital lipodystrophy. BMC Med Genet 2014;15:71.
[7] Kuhara T. Diagnosis and monitoring of inborn errors of metabolism using urease-pretreatment of urine, isotope dilution, and gas chromatography-mass spectrometry. J Chromatogr B Analyt Technol Biomed Life Sci 2002;781:497–517.
[8] Tsurusaki Y, Koshimizu E, Ohashi H, Phadke S, Kou I, Shiina M, et al. De novo SOX11 mutations cause Coffin–Siris syndrome. Nat Commun 2014;5:4011.
[9] Sass JO, Jobard F, Topcu M, Mahfoud A, Werle E, Cure S, et al. L-2-Hydroxyglutaric aciduria: identification of ten novel mutations in the L2HGDH gene. J Inherit Metab Dis 2008;31(Suppl.):S275–9.
[10] Steenweg ME, Jakobs C, Errami A, van Dooren SJ, Adeva Bartolome MT, Aerssens P, et al. An overview of L-2-hydroxyglutarate dehydrogenase gene (L2HGDH) variants: a genotype-phenotype study. Hum Mutat 2010;31:380–90.

ELSEVIER

Brain & Development 37 (2015) 960–966

BRAIN & DEVELOPMENT
Official Journal of the Japanese Society of Child Neurology

www.elsevier.com/locate/braindev

Original article

Mutations in the genes encoding eukaryotic translation initiation factor 2B in Japanese patients with vanishing white matter disease

Shino Shimada [a,b], Keiko Shimojima [a], Noriko Sangu [a,c], Ai Hoshino [d], Yasuo Hachiya [d], Tatsuyuki Ohto [e], Yuichiro Hashi [f], Katsuya Nishida [g], Maki Mitani [g], Saori Kinjo [h], Yoshinori Tsurusaki [i], Naomichi Matsumoto [i], Masafumi Morimoto [j], Toshiyuki Yamamoto [a,*]

[a] *Tokyo Women's Medical University Institute for Integrated Medical Sciences, Tokyo, Japan*
[b] *Department of Pediatrics, Tokyo Women's Medical University, Tokyo, Japan*
[c] *Department of Oral and Maxillofacial Surgery, School of Medicine, Tokyo Women's Medical University, Tokyo, Japan*
[d] *Department of Neuropediatrics, Tokyo Metropolitan Neurological Hospital, Fuchu, Japan*
[e] *Department of Pediatrics, Tsukuba University, Tsukuba, Japan*
[f] *Department of Neurology, National Hospital Organization Kyoto Medical Center, Kyoto, Japan*
[g] *Department of Neurology, National Hospital Organization Hyogo-Chuo National Hospital, Sanda, Japan*
[h] *Department of Pediatrics, Okinawa Chubu Hospital, Uruma, Japan*
[i] *Department of Human Genetics, Yokohama City University Graduate School of Medicine, Yokohama, Japan*
[j] *Department of Pediatrics, Kyoto Prefectural University of Medicine, Kyoto, Japan*

Received 29 September 2014; received in revised form 4 March 2015; accepted 19 March 2015

Abstract

Objective: Vanishing white matter disease (VWM) is a chronic, progressive leukoencephalopathy associated with episodes of rapid deterioration following minor stress events such as head traumas or infectious disorders. The white matter of the patients with VWM exhibits characteristic radiological findings.

Method: The genes encoding all five subunits of eukaryotic translation initiation factor 2B (EIF2B) were analyzed in patients, who were tentatively diagnosed with VWM, by Sanger sequencing.

Results: Seven mutations were identified in the genes encoding the subunits 1, 2, 4, and 5 of EIF2B. Among them, one mutation (p.V83E) in the subunit 2 (*EIF2B2*) was recurrently identified in three alleles, indicating the most common mutation in Japanese patients with VWM. Two patients were homozygous, and the other four patients were compound heterozygous.

Conclusion: All patients showed white matter abnormalities with various degrees. One patient showed manifestations of end-stage VWM disease. Some patients showed late onset and slow progression associated with brain magnetic resonance imaging displaying T2 high intensity only in the deep white matter. There was clinical heterogeneity among patients with VWM.

Keywords: Vanishing white matter disease (VWM); Eukaryotic translation initiation factor 2B (EIF2B); Leukoencephalopathy; Mutation

* Corresponding author at: Tokyo Women's Medical University Institute for Integrated Medical Sciences, 8-1 Kawada-cho, Shinjuku-ward, Tokyo 162-8666, Japan. Tel.: +81 3 3353 8112x24013; fax: +81 3 5269 7667.
E-mail address: yamamoto.toshiyuki@twmu.ac.jp (T. Yamamoto).

http://dx.doi.org/10.1016/j.braindev.2015.03.003

1. Introduction

Childhood ataxia with central hypomyelination (CACH) or leukoencephalopathy with vanishing white matter (VWM; MIM #603896) is a chronic, progressive leukoencephalopathy associated with episodes of rapid deterioration following minor stress events such as head trauma or infectious disorders [1–3]. Patients with VWM show abnormal radiological findings in the brain; i.e., the cerebral white matter appears progressively diffuse and symmetrical abnormalities such as rarefaction and cysts. VWM is an autosomal recessive disease caused by mutations in any of the genes encoding the subunits of eukaryotic translation initiation factor 2B (EIF2B), which is a GTP exchange protein essential for protein synthesis [4,5]. Until now, many disease-causing mutations have been identified [6–16].

In this study, we report on the results of our on-going study to obtain genetic diagnosis for Japanese patients with VWM.

2. Materials and methods

2.1. Patients and samples

This study was approved by the ethics committee at the Tokyo Women's Medical University. After obtaining written informed consents from patients or their families, blood samples were obtained from patients. Patients were recruited under candidate diagnosis of VWM as defined by previously proposed diagnostic criteria by van der Knaap et al. [17]. In the early stages of VWM, white matter involvements may not fulfill the criteria. Therefore, patients who did not show full manifestations but were tentatively diagnosed as VWM were also included in this study. Genomic DNAs were extracted from blood samples using the QIAamp DNA Mini Kit (QIAGEN, Hamburg, Germany). Parental samples were also obtained to confirm inheritance patterns.

2.2. Molecular analysis

All exons of the genes encoding the five subunits of EIF2B (*EIF2B1*, *EIF2B2*, *EIF2B3*, *EIF2B4*, and *EIF2B5*) were genotyped using standard Sanger sequencing. Information on the primers used for this study can be obtained upon request. When heterozygous or homozygous variations were identified in patients, inherited patterns were analyzed using corresponding parental samples. PCR products were subcloned into the pGEM® T-vector (Promega, Madison, WI) to identify the allelic locations of the mutation as described previously [18]. Subsequently, nucleotide sequences of inserted fragments were analyzed in both directions. When a *de novo* mutation was suspected, the biological relationship between the patient and the corresponding parental samples was confirmed by microsatellite marker analysis using the Linkage Mapping Set (Life Technologies, Foster City, CA) as described previously [19].

The identified non-synonymous variants were tested for mutational effects using damaging predication scores obtained from the SIFT [20] (http://sift.jcvi.org/), PolyPhen-2 [21] (http://genetics.bwh.harvard.edu/pph2/), and Combined Annotation-Dependent Depletion (CADD) [22] (http://cadd.gs.washington.edu/info) in accordance with methods reported elsewhere [23]. Interspecies amino acids conservation was checked using the UCSC Genome Bioinformatics Site (https://genome.ucsc.edu/).

3. Results

3.1. Pathogenic mutations

We analyzed a total of 22 patients. Among them, we identified mutations in the genes encoding the EIF2B subunits in six patients including four unrelated individuals and two siblings. All identified mutations were missense mutations (Supplemental Figs. 1 and 2). The results of the molecular analyses in accordance with the clinical information of the patients are summarized in Table 1. Patients 1 and 2 showed homozygous mutations in *EIF2B1* and *EIF2B2*, respectively. Patient 2 was homozygous for p.V83E in *EIF2B2*, and patient 3 had compound heterozygous mutations associated with p.V83E in *EIF2B2*. The other patients showed compound heterozygous mutations in either of *EIF2B2*, *EIF2B4* and *EIF2B5*. Parental origins of all mutations other than p.M305I were confirmed (Table 1). Predicted scores for the deleterious effects of mutations provided by SIFT, Polyphen-2, and CADD are included in Table 1.

Both p.M305I and p.I385T were identified in exon 7 of *EIF2B5* in patient 6. To assess the allelic locations of these two mutations, PCR products were subcloned into the plasmid vector. At least 10 clones were isolated and sequenced. Consequently, all clones showed one of the mutations, indicating that the two mutations were located on the independent alleles. Although p.I385T was identified in the patient's mother, p.M305I was not identified in both parents. We confirmed the biological relationship between patient 6 and his parents by linkage analysis (data not shown).

3.2. Patient reports

Patient 1 is a 61-year-old female, whose parents were cousins. Initial neurological symptoms with gait disturbance were first observed at 29 years of age. At that time, her intellectual quotient was evaluated to be 66. Motor incoordination and spasticity were also noted. Routine laboratory examinations of blood, urine, and

Table 1
Summaries of the clinical information of the patients and the results of mutation analyses.

Patients	Patient 1	Patient 2	Patient 3		Patient 4		Patient 5		Patient 6	
Clinical information										
Gender	F	F	M		M		M		M	
Present age (y/m)	61y	8y	8 m		22y		19y		5y5m	
Onset age (y/m)	29y	3y	8 m		13y		13y		13m	
Provoking event	–	Infection	Infection (fever)		Lack of sleep		Head trauma		Infection (fever)	
Seizure	+	+	+		+		–		+	
Disturbed consciousness	+	+	+		–		+		+	
Other neurological findings	Bedridden	Bulbar paralysis	Spasticity, developmental delay		Mild ataxia		Muscular weakness		Gait disturbance	
Consanguinity	+	–	–		–		–		–	
Family history	–	–	–		The elder brother of Pt. 5		The younger brother of Pt. 4		–	
Identified mutations										
Genes	*EIF2B1*	*EIF2B2*	*EIF2B2*		*EIF2B4*		*EIF2B4*		*EIF2B5*	
Chromosomal location	12q24.31	14q24.3	14q24.3		2p23.3		2p23.3		3q27.1	
Inheritance	Homozygous	Homozygous	Compound heterozygous		Compound heterozygous		Compound heterozygous		Compound heterozygous	
Exon	exon 8	exon 2	exon 2	exon 5	exon 6	exon 11	exon 6	exon 11	exon 7	exon 7
Nucleotide alteration	c.715T>G	c.254T>A	c.254T>A	c.682A>G	c.556T>A	c.1070G>A	c.556T>A	c.1070G>A	c.915G>A	c.1154T>C
Amino-acid change	p.F239V	p.V85E	p.V85E	p.R228G	p.Y186N	p.R357Q	p.Y186N	p.R357Q	p.M305I	p.I385T
Novel/ recurrent	Novel	Recurrent	Recurrent	Novel	Novel	Recurrent	Novel	Recurrent	Novel	Novel
Origin	Not confirmed	Both parents	Paternal	Maternal	Maternal	Paternal	Maternal	Paternal	*de novo*	Maternal
dbSNP build 138	–	–	–	–	–	rs113994033	–	rs113994033	–	–
Damaging prediction										
SIFT score	0.12	0.00	0.00	0.00	0.25	0.15	0.25	0.15	0.13	0.00
SIFT prediction	T	D	D	D	T	T	T	T	T	D
Polyphen2 HVAR score	0.715	0.995	0.995	0.999	0.979	0.637	0.979	0.637	0.196	0.95
Polyphen2 HVAR prediction	P	D	D	D	D	P	D	P	B	D
CADD score (raw)	5.436	5.264	5.264	3.760	4.290	5.227	4.290	5.227	3.735	4.732
CADD score (PHRED-like)	35.0	33.0	33.0	19.1	22.4	33.0	22.4	33.0	19.0	26.4

F, female; M, male; y, years; m, months; Pt., Patient; HVAR, HumVar-trained model autosomal recessive pattern; T, tolerate; D, damaging; B, benign.

cerebrospinal fluid (CSF) showed normal results. Enzyme activities including arylsulfatase A, β-hexosaminidase A, β-mannosidase, and α-fucosidase were within the normal limits. The motor nerve conduction velocity of the left peroneal nerve was 32 m/s, which indicated a delay. Cranial computed tomography showed diffusely distributed low-absorption in the white matter (no more detailed information). Her neurological deterioration progressed, and she is now bedridden. Brain magnetic resonance imaging (MRI) performed at 60 years of age showed diffuse high intensity in the T2-weighted images (Fig. 1).

Patient 2 is an 8-year-old girl. Language developmental delay was noted at 3 years of age. At 7 years, she was admitted to the hospital due to drowsiness after an infectious disease of mycoplasma pneumonia. Due to frequent seizures and respiratory failure, intubation was performed. Brain MRI showed diffuse T2 high

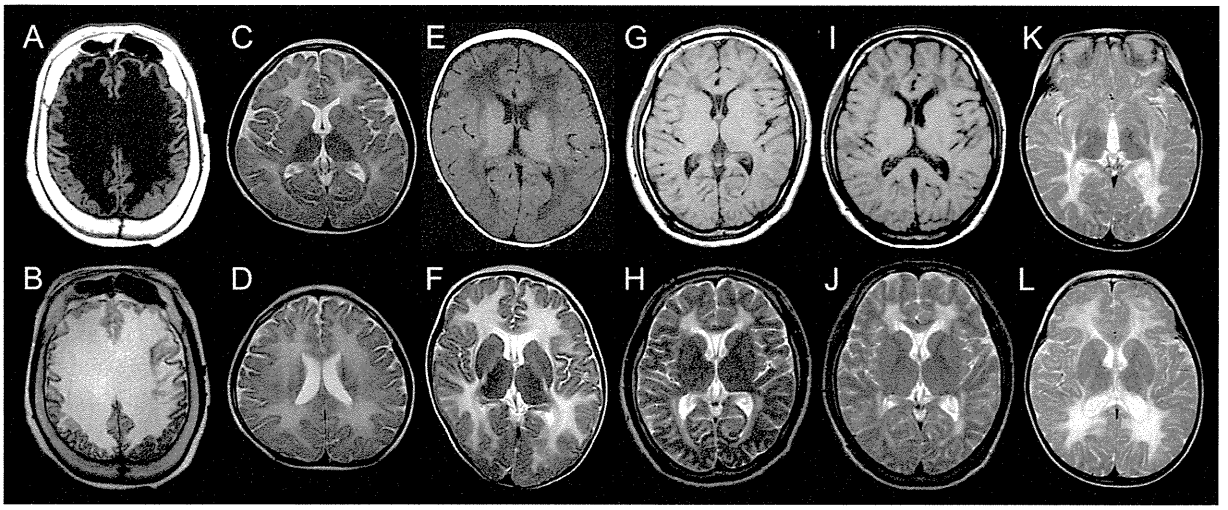

Fig. 1. Brain MRI findings of the patients examined. Axial images show various degrees of abnormal white matter. (A and B) Patient 1 examined at 60 years of age. (C and D) Patient 2 examined at 3 years of age. (E and F) Patient 3 examined at 8 months of age. (G and H) Patient 4 examined at 13 years of age. (I and J) Patient 5 examined at 16 years of age. (K and L) Patient 6 examined at 13 months of age. T1-weighted axial images (A, E, G, and I) and T2-weigthed axial images (B–D, F, H, and J–L). Periventricular zones of patient 1 are not distinguished (A and B). T2-high intensity is only shown in deep white matter, indicating early disease stage in patient 4 and 5 (H and J, respectively).

intensity in the white matter (Fig. 1). Routine laboratory examinations of blood, urine, and CSF showed no abnormality. Her neurological findings have gradually improved. At present, she can speak simple sentences and can walk unassisted.

Patient 3, a baby boy, was born with a weight of 2878 g (25th–50th centile), a length of 49.4 cm (50th–75th centile), and occipitofrontal circumference (OFC) of 33.0 cm (25th–50th centile) at 41 weeks of gestation. At 6 months of age, he showed postnatal growth delay with a weight of 6.2 kg (<3rd centile), a length of 63.4 cm (3rd–10th centile), and OFC of 42 cm (10th–25th centile). Although he showed normal development until 8 months of age, he suddenly displayed drowsiness and poor sucking after an infectious disorder causing high fever, and was admitted to the hospital. At that time, the brain MRI showed diffuse T2 high intensity in the white matter (Fig. 1). Routine laboratory examinations of blood, urine, and CSF, including lactate and pyruvate, showed no abnormality. Screening tests for metabolic disorders of amino acids and very long chain fatty acids also appeared normal. Thereafter, he showed spasticity and severe developmental delay.

Patient 4 is a 22-year-old male, first born from non-consanguineous parents. At the age of 13 years, he started to show epileptic seizures. At that time, brain MRI showed diffuse T2 high intensity in the white matter. Screening tests for metabolic disorders of amino acids and very long chain fatty acids showed normal patterns in patient 4. Enzyme activity of arylsulfatase A and β-galactosidase as well as peripheral nerve conduction velocities, were all within the normal limit. At present, he only shows mild ataxia. Patient 5, the 19-year-old younger brother of patient 4, is the third born among three siblings; his elder sister (the second born) is healthy. Patient 5 also showed a clinical course similar to that of patient 4; he showed epileptic seizures and brain MRI abnormality at age 13 years. When he was 16 years old, a traumatic accident triggered disease progression; he showed prolonged delirium, and then muscular weakness in his left side. Routine laboratory examinations of blood, urine, and CSF showed no abnormality in this sibling case.

Patient 6 is a 3-year and 5-month-old boy. There was no remarkable family or past history. At 13 months, he showed transient drowsiness and gait disturbance two weeks after a febrile convulsion. Brain MRI showed T2 high intensity in the white matter (Fig. 1). After 2 years of age, he easily dropped due to ataxic gait. At present, his height is 95.1 cm (25th–50th centile), weight is 15.9 kg (75th–90th centile), and OFC is 51.8 cm (90th–97th centile). He cannot stand alone due to spasticity in his lower extremities. Compared to motor development, his cognitive development was within the normal limit. Screening tests for metabolic disorders of amino acids and very long chain fatty acids showed normal patterns. Enzyme activities including arylsulfatase A, β-hexosaminidase A, β-galactosidase, galactosylceramidase were within the normal limits. There were no mutations in the glial fibrillary acidic protein gene (*GFAP*) nor the megalencephalic leukoencephalopathy with subcortical cysts 1 gene (*MLC1*).

4. Discussion

In this study, a molecular diagnosis of VWM was established in six patients from five families (Table 1). All of the identified mutations are depicted in the

primary structures of EIF2B genes together with previously reported mutations (Fig. 2) [4–16]. The damage prediction scores of the identified mutations were calculated and summarized in Table 1. Although the some of the predictions from SIFT and Polyphen-2 appeared benign or tolerated, all CADD scores (PHRED-like) were higher than 15. Thus, mutations identified in this study likely to have pathogenic effects.

In patient 6, p.I385T was inherited from his mother; however, p.M305I was not identified either parent. Therefore, p.M305I was suspected to be of *de novo* origin in the paternally derived allele. The UCSC Genome Bioinformatics Site displays the different single nucleotide polymorphisms (SNPs) in the same residues, p.M305L (rs200143780) and p.I385V (rs113994073) (Supplemental Fig. 2). The p.I385V is registered as a "flagged" SNP and has previously been reported as pathogenic [24] (Fig. 2). Compared to this, p.M305L is not shown as a "flagged" in the database; however, the minor allele frequency (MAF) of p.M305L is reported to be as low as 0.050% (1/2000). Because VWM is caused by an autosomal recessive trait, existence of only one individual with heterozygosity of p.M305L among 1000 normal populations may suggest that this individual is a healthy carrier of this possibly disease-causing variant. Therefore, existence of the different SNP of this residue (p.M305L) in the database does not deny pathogenesis of p.M305I. These findings indicate that these two variants are likely deleterious.

Among the 10 alleles present in the five families, three alleles (30%) shared the p.V85E mutation in *EIF2B2*. Previously, p.V85E has been identified in Japanese

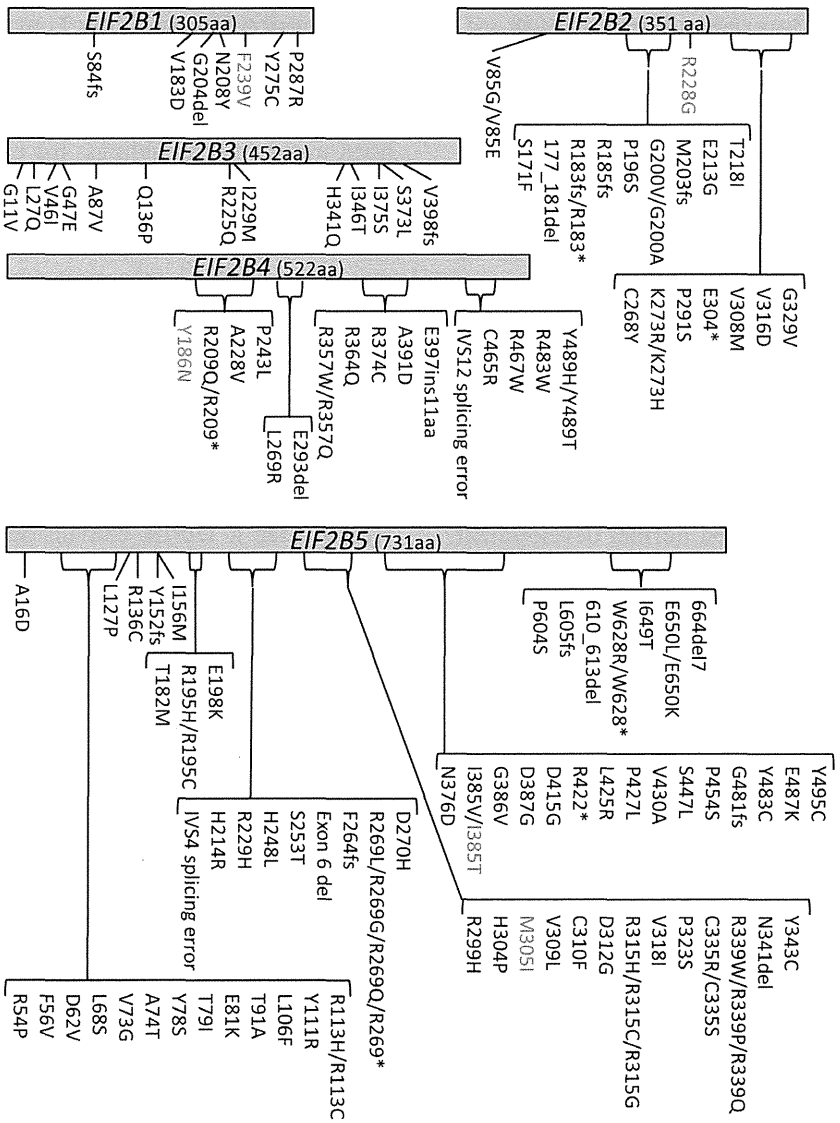

Fig. 2. Schematic representation of the distribution of EIF2B gene mutations. The novel mutations identified in this study are depicted on the primary structures of EIF2B genes in red characters, while known mutations are shown in black. (For interpretation of the references to color in this figure legend, the reader is referred to the web version of this article.)

patients [25]. We also reported this mutation in a patient with VWM, which was unmasked by a microdeletion of the homologous allele [26]. Therefore, this mutation is most common in the Japanese population. Because p.V85E has also identified in a Chinese patient [13], this variant may be common in individuals of east Asian origin. Other than p.V85E in *EIF2B2*, p.R357Q in *EIF2B4*, registered as rs113994033, was recurrently identified in the literature [8]. The other five mutations identified in this study were novel and have not been reported previously (Table 1). Due to the limited number of patients, we were unable to identify any genotype–phenotype correlation.

In this study, patient 1 at 61 years of age presented clinical manifestations of the end stage of VWM, with completely vanishing white matter. We are unable to distinguish the border of periventricular zones in the brain MRI for this patient. Although patient 1 is now bedridden with no response or motor activity, the onset of her neurological symptoms began at age 29. Therefore, compared to the other patients, this patient showed later onset of disease and slower disease progression. The sibling case of patient 4 and 5 also showed late onset and slow progression, and only started to exhibit neurological symptoms after adolescence. In the early stage of VWM, brain MRI may not necessarily show diffuse cerebral white matter abnormalities and rarefaction or cystic degeneration [27]. Therefore, the brain MRI of patient 4 and 5, showing abnormal T2 high intensity only in the deep white matter, is suggestive of an early disease stage.

The other three patients (patient 2, 3, and 6) showed typical, diffuse white matter abnormalities in MRI. They started to show neurological symptoms during early infancy, and their disease occurrences were triggered by environmental factors (high fever due to infections) and were followed by episodes of acute deterioration associated with disturbed consciousness and seizures. These provocations have been frequently observed in VWM patients [11].

Because EIF2B is involved in regulating the first steps of protein synthesis and is ubiquitously expressed, it is unclear why EIF2B alterations cause a brain-specific disease [28,29]. Although many mutations identified in patients with VWM showed reduced EIF2B activities [30], basal activities *per se* do not explain the disease severity. Rather, the decreased EIF2B activity might impair the cellular stress response and improperly activate the unfolded protein response (UPR) leading to the endoplasmic reticulum (ER) stress [31]. The ER load in astrocytes and oligodendrocytes is possibly higher than in other cell types, rendering them vulnerable to conditions that predispose to ER stress [32,33]. This is the probable reason for disease provocations after environmental stress factors in patients with EIF2B alterations.

In this study, we recruited 22 patients who showed mimicking clinical manifestations of VWM. Among them, only six patients had genomic mutations in EIF2B genes. The final diagnosis of the other 16 patients is unknown at present. This would be challenges to be overcome in our future.

Acknowledgements

We would like to acknowledge the Collaborative Research Supporting Committee of the Japanese Society of Child Neurology (14-3) for promoting this study. This work was supported by a Grant-in-Aid for Scientific Research from Health Labor Sciences Research Grants from the Ministry of Health, Labor, and Welfare, Japan (T.Y.).

Appendix A. Supplementary data

Supplementary data associated with this article can be found, in the online version, at http://dx.doi.org/10.1016/j.braindev.2015.03.003.

References

[1] van der Knaap MS, Barth PG, Gabreels FJ, Franzoni E, Begeer JH, Stroink H, et al. A new leukoencephalopathy with vanishing white matter. Neurology 1997;48:845–55.
[2] Hanefeld F, Holzbach U, Kruse B, Wilichowski E, Christen HJ, Frahm J. Diffuse white matter disease in three children: an encephalopathy with unique features on magnetic resonance imaging and proton magnetic resonance spectroscopy. Neuropediatrics 1993;24:244–8.
[3] Schiffmann R, Moller JR, Trapp BD, Shih HH, Farrer RG, Katz DA, et al. Childhood ataxia with diffuse central nervous system hypomyelination. Ann Neurol 1994;35:331–40.
[4] Leegwater PA, Vermeulen G, Konst AA, Naidu S, Mulders J, Visser A, et al. Subunits of the translation initiation factor eIF2B are mutant in leukoencephalopathy with vanishing white matter. Nat Genet 2001;29:383–8.
[5] van der Knaap MS, Leegwater PA, Konst AA, Visser A, Naidu S, Oudejans CB, et al. Mutations in each of the five subunits of translation initiation factor eIF2B can cause leukoencephalopathy with vanishing white matter. Ann Neurol 2002;51:264–70.
[6] Pronk JC, van Kollenburg B, Scheper GC, van der Knaap MS. Vanishing white matter disease: a review with focus on its genetics. Ment Retard Dev Disabil Res Rev 2006;12:123–8.
[7] Maletkovic J, Schiffmann R, Gorospe JR, Gordon ES, Mintz M, Hoffman EP, et al. Genetic and clinical heterogeneity in eIF2B-related disorder. J Child Neurol 2008;23:205–15.
[8] Scali O, Di Perri C, Federico A. The spectrum of mutations for the diagnosis of vanishing white matter disease. Neurol Sci 2006;27:271–7.
[9] Matsui M, Mizutani K, Ohtake H, Miki Y, Ishizu K, Fukuyama H, et al. Novel mutation in EIF2B gene in a case of adult-onset leukoencephalopathy with vanishing white matter. Eur Neurol 2007;57:57–8.
[10] Horzinski L, Gonthier C, Rodriguez D, Scherer C, Boespflug-Tanguy O, Fogli A. Exon deletion in the non-catalytic domain of eIF2Bepsilon due to a splice site mutation leads to infantile forms of CACH/VWM with severe decrease of eIF2B GEF activity. Ann Hum Genet 2008;72:410–5.